Contents lists available at ScienceDirect

Engineering Structures

journal homepage: www.elsevier.com/locate/engstruct

Numerical study of the flange buckling behavior of trapezoidally corrugated web girders

Amr E.K. Qureshi [a,*], Sedky A. Tohamy [b], Amr B. Saddek [c,d], Ahmed A.M. Drar [e]

[a] Civil Engineering Department, Sohag University, Egypt
[b] Civil Engineering Department, Minia University, Egypt
[c] Civil Engineering Department, Albaha University, Saudi Arabia
[d] Civil Engineering Department, Beni-Suef University, Egypt
[e] Civil Engineering Department, Sohag University, Egypt

ARTICLE INFO

Keywords:
Bending behavior
Flange local buckling coefficient
Corrugated web
ABAQUS/CAE

ABSTRACT

Trapezoidal corrugated web steel plate girders (TCWPGs) are heavily considered as advanced structural elements in the structural engineering branch due to their many advantages. However, not many researchers focused on studying the calculation of the capacity of these girders under bending moment and the bending behavior of these girders when it fails by flange local buckling of the slender compression flange. In this paper, an intensive parametric study has been performed on trapezoidal corrugated web girders subjected to pure bending moment to investigate and analyze the flange local buckling coefficient. Flange slenderness ratio, web slenderness ratio, flange-to-web thicknesses ratio and the trapezoidal web enclosing effect were investigated numerically to study and analyze their effect on the coefficient of local flange buckling in this type of girders. Also bending moment resistance of these girders has been studied. The behavior of these girders has been investigated using ABAQUS FE software. A criterion of the Egyptian code for classifying the compression flanges has been found to be suitable to be used for studying the effect of web thickness on the bending moment resistance of trapezoidal web girders. Depending on the shape of the web corrugations, it is specified if the compression flange slenderness should be depending on the average outstand distance or the maximum outstand distance. Also, some important advices have been introduced for the economic and safe design of these girders to be taken in designers' consideration.

1. Introduction

The corrugated web girders are formed by welding two flat plates (upper and lower flanges) with corrugated web plate. They are used as good structural elements in the construction of steel bridges, frames and columns of buildings. The plate girders with trapezoidal corrugated web shown in Fig. 1 have been considered as the most economical and spreading type of girders in steel bridges construction even today as it consumes less amount of steel material due to using of thinner web when compared to flat web girders. It has been concluded from previous studies on corrugated web girders that the corrugated web girders has higher shear capacity more than the shear capacity of flat web girders having the same web thickness [1]. Also, lower cost has been achieved after manufacturing these girders due to less maintenance processes carried. The flexural behavior of plate girders with corrugated web had been studied by some researchers in the literature also the flange local buckling behavior (FLB) in these girders had been studied in the last twenty years. Some aspects concerned to the flexural behavior were studied in an analytical, experimental, and numerical manner. The ultimate bending strength, flange local buckling, lateral-torsional buckling (LTB), and linear elastic response had been included in these aspects.

Johnson and Cafolla [3] conducted an investigation on local buckling of flange. They conducted a numerical parametric study to specify a proper flange outstand width to be used in the calculation of the elastic flange local buckling capacity in trapezoidal web steel girders. A wide compression flange had been independently modeled. The effect of web corrugations had been simulated by rigid restraints introduced into the flange. They identified a non-dimensional parameter (R) given by **Eq. (1)**.

$$R = \frac{(a_1 + a_4)a_4.tan\theta}{(a_1 + 2a_4)b_f} \quad (1)$$

They conducted an experimental test on five specimens, three of

* Corresponding author.
E-mail addresses: Amr.el_sayed@eng.sohag.edu.eg (A.E.K. Qureshi), amro@bu.edu.sa, amr01174@eng.bsu.eg (A.B. Saddek).

https://doi.org/10.1016/j.engstruct.2021.113120
Received 16 June 2020; Received in revised form 22 April 2021; Accepted 30 August 2021

Nomenclature

b_f	flange width	a_4	horizontal projection of the inclined panel width of the corrugated web
t_f	flange thickness	θ	corrugation angle
h_w	corrugated web height	E	modulus of elasticity of steel
t_w	corrugated web thickness	σ_{cr}	critical compressive stress
C_f	large flange outstand = $(b_f + a_3)/2$	$\sigma_{cr,FEM}$	critical stress obtained by finite element analysis
a	buckling length of the compression flange sub-panel = $a_1 + a_4$	u	initial imperfection magnitude
		P_{cr}	critical load
R	enclosing effect of the trapezoidal corrugated web	υ	Poisson's ratio
a_1	web horizontal panel width	k	buckling coefficient
a_2	web inclined panel width	α	flange sub-panel aspect ratio = C_f/a
a_3	corrugation depth	λ	slenderness ratio (length/thickness ratio)

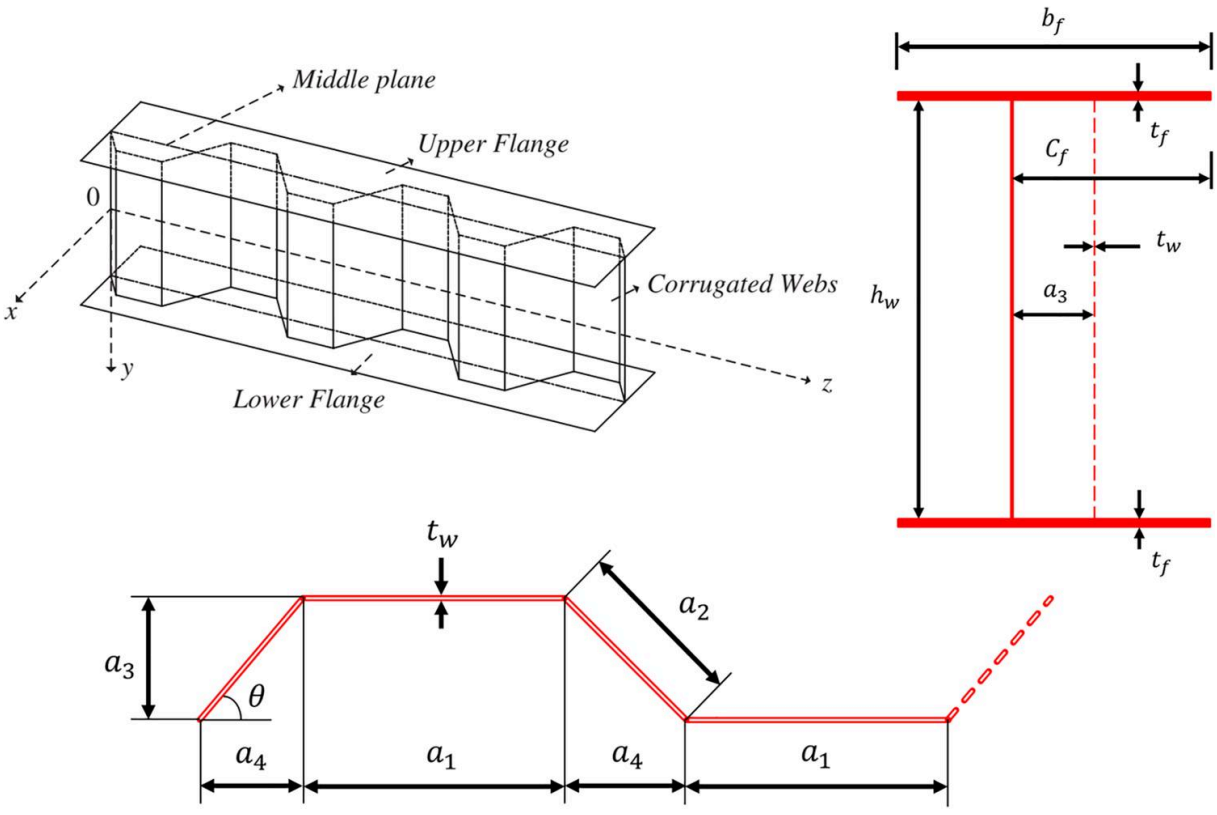

Fig. 1. Trapezoidal profile of web and geometric properties [2].

them failed by local buckling of flange and web shear buckling was noticed in the other two specimens. Elgaaly et al. [4] tested six corrugated web girders under uniform bending moment. The failure mode of their specimens was the inelastic buckling of the compression flange. Five of specimens suddenly failed due to yielding of the compression flange then vertical inelastic buckling of the flange into the web had been occurred.

Y.A. Khalid et al. [5] investigated the web corrugation effect on the capacity of corrugated web beams. Flat web beams and beams with horizontally corrugated and vertically corrugated webs had been investigated using LUSAS finite element software. In the horizontally corrugated case, one arc and two arcs were studied, while a corrugation of half-circular wave had been utilized for the vertical type. For each type of the beam, three different corrugation radii had been taken to study the effect of corrugation radius on the beam's resistance. Beams, with flat web, had been also tested by test experiments. Also, it had been found that beams with vertically corrugated web give 38.8% to 54.4% higher strength of bending moments than beams with horizontally corrugated web. The vertically corrugated web provides stronger resistance against buckling of flange, compared to beams with flat web and beams with horizontally corrugated web. The same results had been obtained for the three radii studied. Also, beams with larger radius of corrugation in the corrugated web could give higher capacity of bending moment. Also they stated that by using the vertical-corrugated web, a reduction in weight could be achieved.

Dabon and Elamary [6] conducted an experimental investigation on four specimens exposed to bending. Two specimens were flat and corrugated web with non-compact flange. Compact flanges were used in the other two specimens. The effect of compactness of the flange on the behavior of corrugated web beams had been analytically and experimentally studied. Beams with corrugated webs had been compared to those with flat webs to specify the advantages and disadvantages of

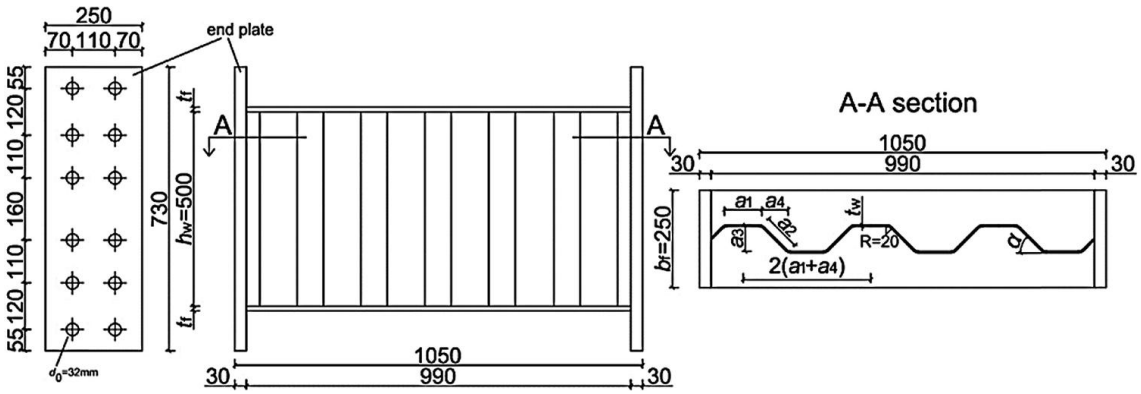

Fig. 2. Used geometrical properties of trapezoidal corrugated web girders [13].

using corrugated web. The results showed that; the beam yield load had been enhanced by the flange transversal stiffeners by 21% and the flange thickness increased the yield load by 56%. If both of them used, 72% of the beam yield load could be achieved if these enhancement existed in these beams. Watanabe and Masahiro [7] declared the results of the experimental test of girders with corrugated web subjected to pure bending moments. Four different corrugations of trapezoidal profiled web and one flat web profile have been used in their test. The failure mode which noticed in all girders was the local buckling of the compression flange. They compared the test results of ultimate strength and bending behavior with the results of numerical study using DIANA FE software. Sayed-Ahmed [8] conducted a linear buckling parametric analysis to investigate the flange local buckling in corrugated web girders. A 0.7 limit of the coefficient of buckling has been concluded in the results of the analysis and the larger flange outstand should be used in the compression flange classification. Numerical investigation had been done on the local buckling behavior of the compression flange in corrugated web girders. Leong and Osman [9] studied three plates failed by flange local buckling phenomena. The trapezoidal profile of the corrugated web welded to the flange had been studied on the flange subjected to compression.

Slender trapezoidal web specimens had been tested experimentally by Lho et al. [10]. They aim to study the estimation of the maximum slenderness ratio of the profiled web to prevent the occurrence of the induced buckling failure type of the compression flange. Also they conducted a linear buckling analysis and based on the experimental results of their test they concluded that, the profiled web's maximum ratio of slenderness could be 1.5 times higher than the slenderness ratio of the DASt-Richtlinie 015 [11]. Experimental and numerical investigations of six specimens with wide flanges subjected to normal force and bending moment at the same time have been studied by Li et al. [12]. The aim of their study was the calculation of outstand-to-thickness ratio limit of the compression flange using linear buckling analysis, and then the classification limit was modified through nonlinear finite element analysis considering the geometrical imperfections and residual stresses effect. Parametric studies had been carried out to study local buckling strength of the compression flange affected by the corrugated web, tension flange and the length of the beam. FE model has been used to study the effect of the initial geometric imperfection of the compression flanges and residual stresses on the critical buckling stress. It was concluded that the critical buckling stress reduced by 28% due to the initial imperfections effect, while residual stresses reduced it by 14%. A 70% correction factor was recommended for the critical outstand-to-thickness ratio of the flanges to consider these two effects in the stability of beams with corrugated webs.

B. Jáger et al. [13] carried out an experimental investigations on 16 specimens of trapezoidally corrugated web girders simply supported and subjected to four-point-bending to investigate the phenomenon of local buckling of the flange and calculate the bending resistance of the tested girders. The failure mode of all specimens was local buckling of the compression flange, however, two different failure modes can be noticed based on results of the test. In case of higher values of flange-to-web thickness ratio ($t_f/t_w > 2.5$) the flange rotated unrestrictedly around the corrugated web. On the other side in case of lower values of flange-to-web thickness ratio ($t_f/t_w < 2.5$) the failure made was separated buckling of the compression flange subpanels bounded by the profile of corrugated web. Combined buckling mode was observed from the test results. They also concluded that the profile of web corrugation has a large effect on the flange initial geometric imperfection and the magnitude of initial imperfection is influenced by the largest flange outstand to thickness ratio. In their numerical investigations [14] an advanced FE model was developed and validated. They studied a sensitivity analysis of the imperfection to develop proposals for equivalent geometric imperfections to be applied in the FEM based design method. They also carried out a parametric study to improve the calculation of the buckling coefficient of the compression flange in corrugated web girders.

The previous studies show, that a small number of the available studies done by literature investigated the bending behavior of steel corrugated web girders and the flange buckling capacity in trapezoidal corrugated web girders (TCWPGs). Also not many researchers studied the full behavior of these girders in bending by taking wide range of girders dimensions used in real-world steel bridges. In the current study, an extensive numerical parametric study is used to give an explanation for the bending behavior of trapezoidal web girders. Also based on the results obtained by the numerical solution, some guidelines have been recommended to be considered in the design of the trapezoidal corrugated web girders.

2. FE model development and validation

2.1. General

The commercial software of finite element modelling ABAQUS/CAE [15] has been used in current study. The simulation consists of two types of analysis. The first analysis is the linear buckling analysis (LBA), it has been conducted on a perfect corrugated web girder to obtain its modes of buckling which have been utilized as initial imperfection shape of the I-girder. Also local buckling coefficient of the compression flange has been obtained. The second analysis is the nonlinear analysis with imperfect geometrical and material behavior (GMNIA) in which the concentrated loads have been applied in small increments using the modified RIKS method available in the software library. The modified RIKS method is a load–deflection analysis generally used to predict unstable, geometrically nonlinear collapse of a structure as it can include nonlinear materials and boundary conditions.

Experimental data of B. Jáger et al. [13] were used to obtain the numerical model to be investigated in the numerical parametric study.

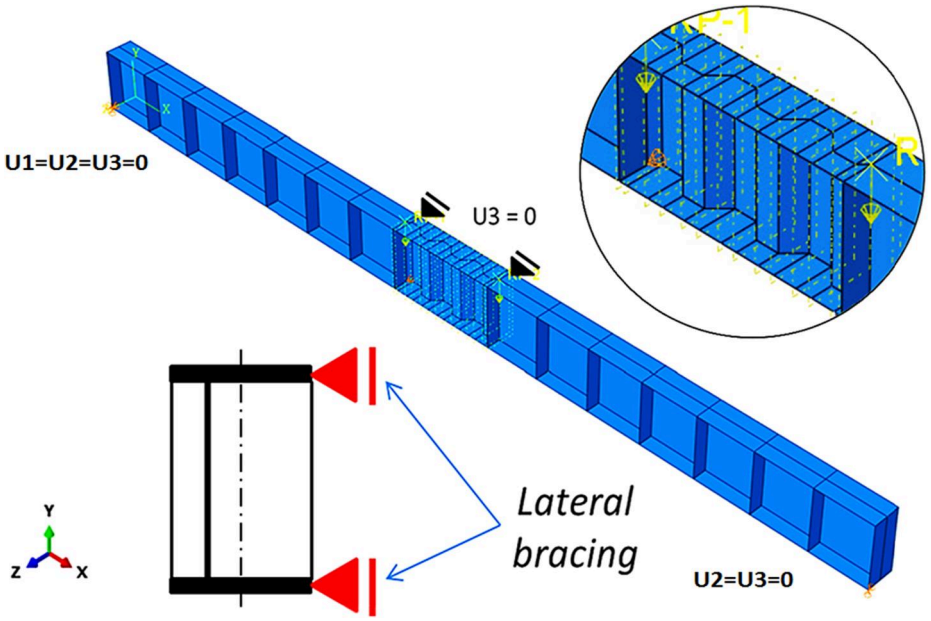

Fig. 3. Supports restraints and lateral bracing in 3D finite element model.

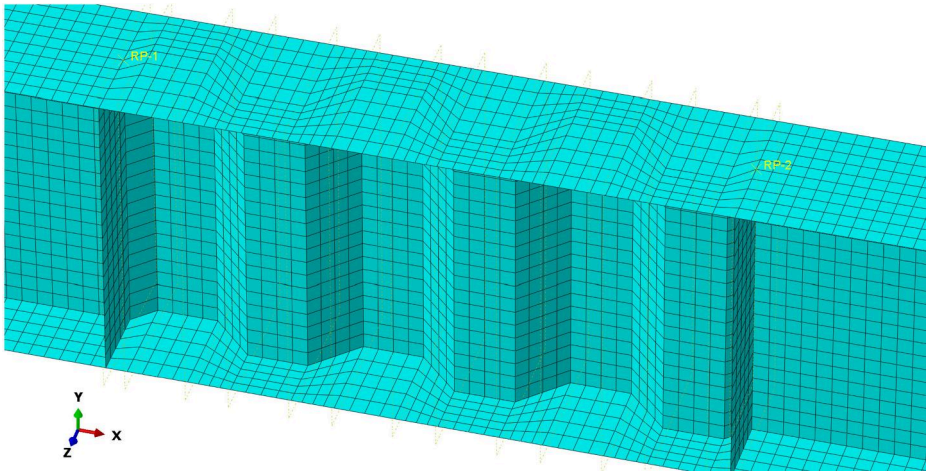

Fig. 4. Mesh used in the finite element model.

To check the FE model validity, a comparison between the results of the experimental test and the numerical analysis results has been made. Their test was a four-point bending loading test on 16 large scale simply supported specimens. Ten girders having four different trapezoidal profile geometries have been tested. The material and geometrical properties of the tested girders were declared by Jáger [13]. All tested girders have 250 mm nominal flange width, and 500 mm depth of corrugated web. The used notations are shown in Fig. 2.

2.2. Boundary conditions, load points, and lateral constraints

The used boundary conditions in the current finite element model were pin support on one side of the girder where the restrained displacements were in x-, y-, z-directions and the other side has roller support where the restrained displacements were in y-, z-directions. Two concentrated loads have been statically applied at start and end of the middle third of the girder. Vertical stiffeners have been located in the model at the locations of the concentrated loads and support reactions. These stiffeners have been located on the girder to prevent the flange local crippling where the web was welded. To prevent the failure of girders by the lateral-torsional buckling mode, the FE models have been constrained laterally at the application points of the two concentrated loads. Fig. 3 presents the experimental layout of girders tested by B. Jáger et al. [13] which considered in the FE model of the current study.

2.3. Element type and meshing

A 4-node doubly curved thin or thick shell, reduced integration, hourglass control, finite membrane strains (S4R) element was used in the current study as it is the most used element suitable for modelling of built up steel girders. S4R element from the element library has been used to discretize the flanges, web and the vertical stiffeners. The S4R element is suitable for complex buckling behavior. Each node of this element has six degrees of freedom. At each node there are three translational degrees of freedom and three rotational degrees of freedom. Finite membrane strains and arbitrarily large rotations could be accounted for using this element. So, large strain analyses and nonlinear geometrical problems can be solved. Fig. 4 shows the mesh used in the current FE model.

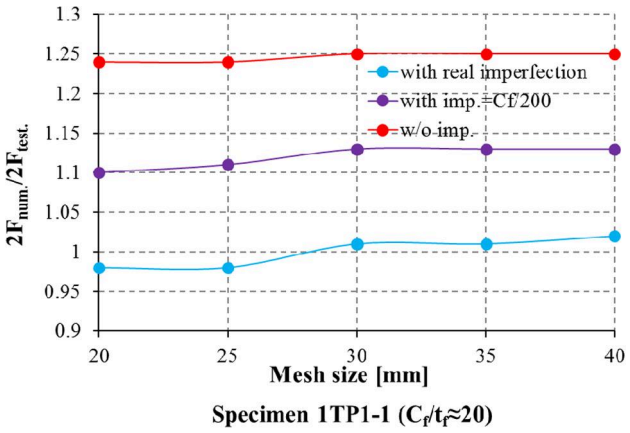

Fig. 5. Convergence study of mesh size and initial imperfection magnitude.

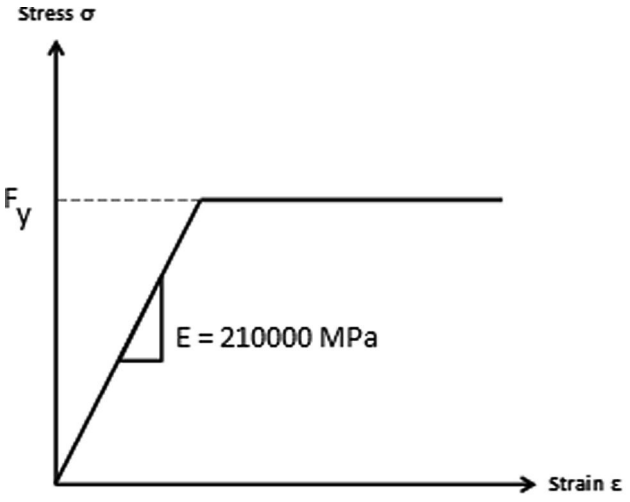

Fig. 6. Elastic-perfect plastic stress–strain curve used in FE model.

2.4. Convergence study

Convergence study is performed to investigate the suitable size of mesh to be used in the numerical model to get accurate and converged results. In Fig. 5 the results of convergence study were presented and plotted at various imperfection magnitudes. Relationship between the numerical to experimental total applied load ratio on the vertical axes and the mesh size on the horizontal axes is plotted at various values of initial imperfection magnitudes. In this study a mesh size of 30 mm was considered as the best size to get accurate results and save the computation time also.

2.5. Material properties

Steel 36/52 [16] has been assumed to be used in this study. The behavior of steel was considered as elastic-perfect-plastic without strain hardening. It has been concluded by Hassanein et al. [17] that the differences in results between elastic-perfect plastic and elastic–plastic with strain hardening models were 3.5%, based on their comparison, the elastic-perfect plastic stress–strain curve was used in their study. In the current study, the stress–strain curve of the used steel has been shown in Fig. 6. In the linear stage of the analysis, steel modulus of elasticity has been evaluated to be 210000 MPa, steel Poisson's ratio equals 0.3 and yield stress of 360 MPa was considered.

2.6. Modelling of equivalent geometrical imperfections

To get an accurate numerical analysis and obtain real results, the equivalent geometrical imperfections should be added to the FE models before performing the nonlinear numerical analysis. In the nonlinear analysis, equivalent imperfections have been introduced using the perturbations in the geometry. Geometrical imperfections were added onto the "perfect'' FE model to create out-of-plane displacements of the plate elements. A two-step method for modelling corrugated web girder having equivalent imperfections. In the first step, the elastic buckling analysis has been carried out on a perfect mesh to generate the expected modes of buckling and the nodal displacements of these buckling modes. In the second step, applying the geometrical imperfections to the perfect mesh has been done by adding the first positive elastic buckling mode in Fig. 7 to the perfect mesh in the FE modelling with scaling factor equal to the equivalent imperfection amplitude.

The EN1993-1-5 [18] suggested equivalent geometric imperfection magnitude for flanges subject to twist equals $C_f/50$, where C_f is the largest outstand distance of the compression flange. This value was considered by B. Jáger et al. [14] for simulating the initial geometric imperfections and residual stresses of trapezoidal corrugated web girders. This value has been selected in the current parametric study to

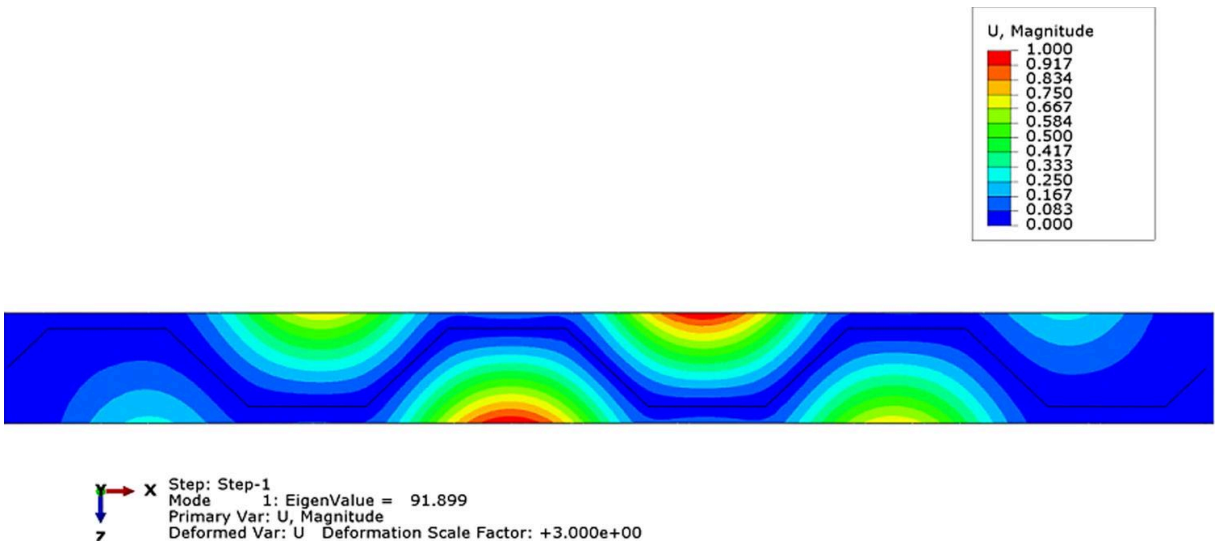

Fig. 7. First positive eigen-mode.

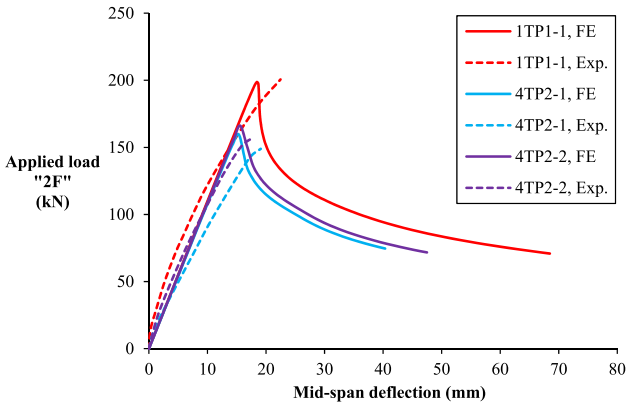

Fig. 8. Curves of load vs mid-span displacement for test specimens.

Table 1
Comparison between numerical and experimental load carrying capacities.

No.	Specimen	2F (Exp.) kN	2F (Num.) kN	Difference %
1	1TP1-1	200.5	198.7	0.9
2	4TP2-1	148.7	159.3	7.1
3	4TP2-2	156.3	166.2	6.3
4	5TP2-1	172.1	194	12.8
5	8TP2	306.2	297.4	2.9
6	9TP3	326.3	314.9	3.5

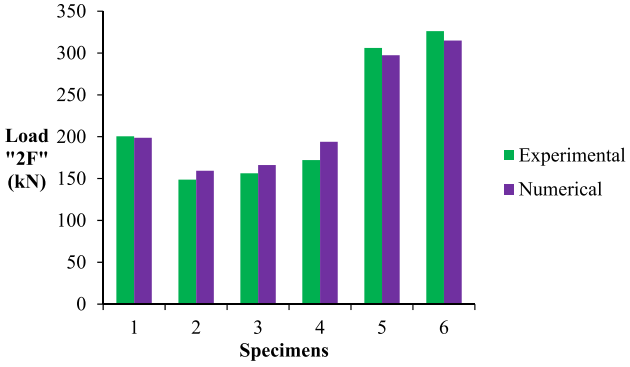

Fig. 9. Comparison between numerical and experimental load carrying capacities.

take the initial geometrical imperfections and residual stresses effect into account [14].

2.7. Validity of the FE models

The results of this validation have been indicated as the total load versus the mid-span deflection of test specimens. A comparison of verified girders has been made as shown in Fig. 8.

The small differences in the deflection of girders between the experimental and the numerical analysis were noticed due to using the first positive buckling mode as initial imperfection shape instead of using the real imperfection shape of the flange. Comparison between the results of the experimental and the numerical load carrying capacities is summarized in Table 1 and indicated in Fig. 9.

Only 6 specimens were used for model validation from the 16 specimens of Jáger et al. because the authors could not extract the imperfection amplitudes declared by Jáger et al. except for these specimens. The initial imperfection magnitudes have a large effect on the accuracy of the results of FE model, however, the imperfection amplitudes of each specimen have not been declared by B. Jáger et al. [13]. In Table 1, **12.8**% difference between the experimental and numerical total applied load of 5TP2-1 specimen may referred to non-declared magnitude of initial imperfection of this specimen definitely. Previous comparisons between the results of the experimental test and the numerical analysis results from the finite element modelling explain that the numerical model presented in the finite element simulations is suitable to be considered in the numerical study. The results of the validation of the FE model explain a good agreement with the experimental data as shown in Fig. 10.

3. Numerical parametric study

Geometric properties and parameters

The analytical model used in the current study consists of a simply supported girder subjected to two point load at third points as shown in Fig. 11. The most extreme layouts of the parameters have been selected to study the full behavior of the considered girders. In the current numerical analyses, the following parameter ranges were investigated and analyzed:

$t_f = 8, 12, 14, 16, 20, 24$ mm
$h_w/t_w = 125 \sim 500$
$t_f/t_w = 1 \sim 12$
$C_f/t_f = 6.25 \sim 31.875$

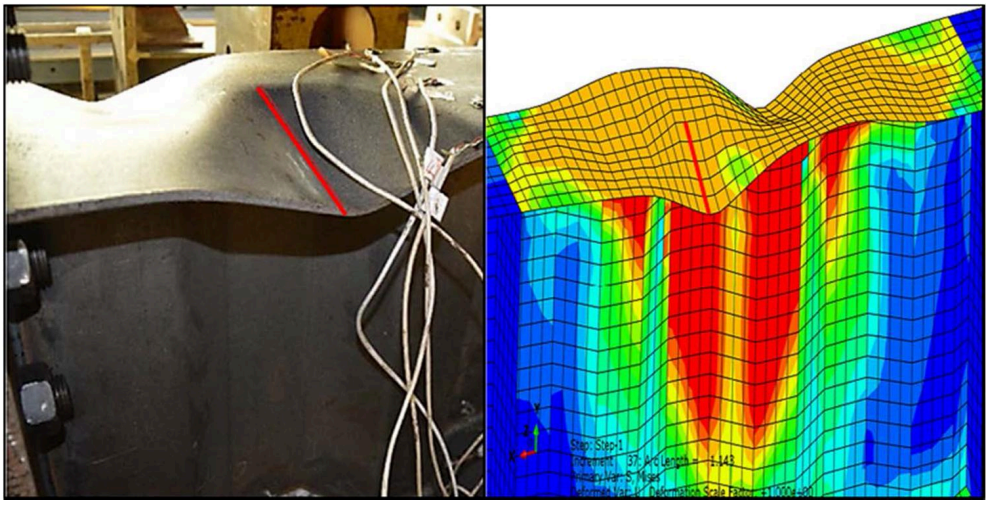

Fig. 10. Experimental vs. Numerical failure mode [13].

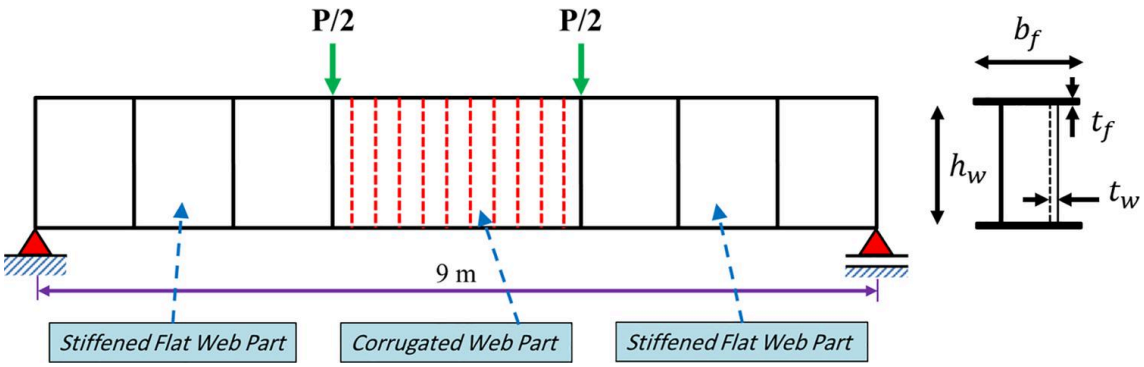

Fig. 11. Geometry of trapezoidal corrugated girder under four-point bending loading.

Table 2
Models used in the parametric study.

Groups	Models	h_w (mm)	t_w (mm)	b_f (mm)	t_f (mm)	$a_{1,2}$ (mm)	a_3 (mm)	a_4 (mm)
A	MTR16A1	1000	8	300	16	40	30	30
	MTR16A2	1000	8	300	16	70	50	50
	MTR16A3	1000	8	300	16	100	70	70
	MTR16A4	1000	8	300	16	150	105	105
	MTR16A5	1000	8	300	16	170	120	120
	MTR16A6	1000	8	300	16	200	140	140
	MTR16A7	1000	8	300	16	220	155	155
	MTR16A8	1000	8	300	16	250	175	175
	MTR16A9	1000	8	300	16	300	210	210
B	MTR16B1	1000	6	300	16	40	30	30
	MTR16B2	1000	6	300	16	70	50	50
	MTR16B3	1000	6	300	16	100	70	70
	MTR16B4	1000	6	300	16	150	105	105
	MTR16B5	1000	6	300	16	170	120	120
	MTR16B6	1000	6	300	16	200	140	140
	MTR16B7	1000	6	300	16	220	155	155
	MTR16B8	1000	6	300	16	250	175	175
	MTR16B9	1000	6	300	16	300	210	210
C	MTR16C1	1000	4	300	16	40	30	30
	MTR16C2	1000	4	300	16	70	50	50
	MTR16C3	1000	4	300	16	100	70	70
	MTR16C4	1000	4	300	16	150	105	105
	MTR16C5	1000	4	300	16	170	120	120
	MTR16C6	1000	4	300	16	200	140	140
	MTR16C7	1000	4	300	16	220	155	155
	MTR16C8	1000	4	300	16	250	175	175
	MTR16C9	1000	4	300	16	300	210	210
D	MTR16D1	1000	2	300	16	40	30	30
	MTR16D2	1000	2	300	16	70	50	50
	MTR16D3	1000	2	300	16	100	70	70
	MTR16D4	1000	2	300	16	150	105	105
	MTR16D5	1000	2	300	16	170	120	120
	MTR16D6	1000	2	300	16	200	140	140
	MTR16D7	1000	2	300	16	220	155	155
	MTR16D8	1000	2	300	16	250	175	175
	MTR16D9	1000	2	300	16	300	210	210

Note: MTR16A1: M refers to model, TR refers to trapezoidal corrugated web, 16 refers to $t_f = 16$ mm, A refers to web slenderness ratio ($h_w/t_w = 125$), B refers to web slenderness ratio ($h_w/t_w = 167$), C refers to web slenderness ratio ($h_w/t_w = 250$), D refers to web slenderness ratio ($h_w/t_w = 500$), and from 1 to 9 refers to web corrugation profile.

$R = 0.07 \sim 0.5$
$b_f/a_3 = 1.4 \sim 10$

In the FE models of current study, the applied geometric ranges of the corrugation profile were the angle of corrugation equals 45^0 and $a_1 = a_2$ ranges from 40 to 300 mm to get the extreme values of the layout of girders profile. Also t_f ranges from 8 mm to 24 mm. It was considered that h_w should be constant with changing of t_w to get various web slenderness ratios. In the current parametric study, almost 240 different geometries have been investigated to study the selected range of the parameters. Some of the models have been indicated in Table 2.

4. Results and discussion

Using the linear analysis of buckling, flange local buckling coefficient has been calculated using the critical load multiplier. Since the critical normal stresses in the flange were determined by assuming that the flange normal stress distribution is uniform along the flange width instead of assuming non-uniform normal stress distribution in the flanges as simplified and conservative solution. The strains measurements conducted by Jáger [13] prove that this assumption is applicable if only the bending moments were applied on the corrugated web girder. The numerical local buckling coefficient of compression flange was

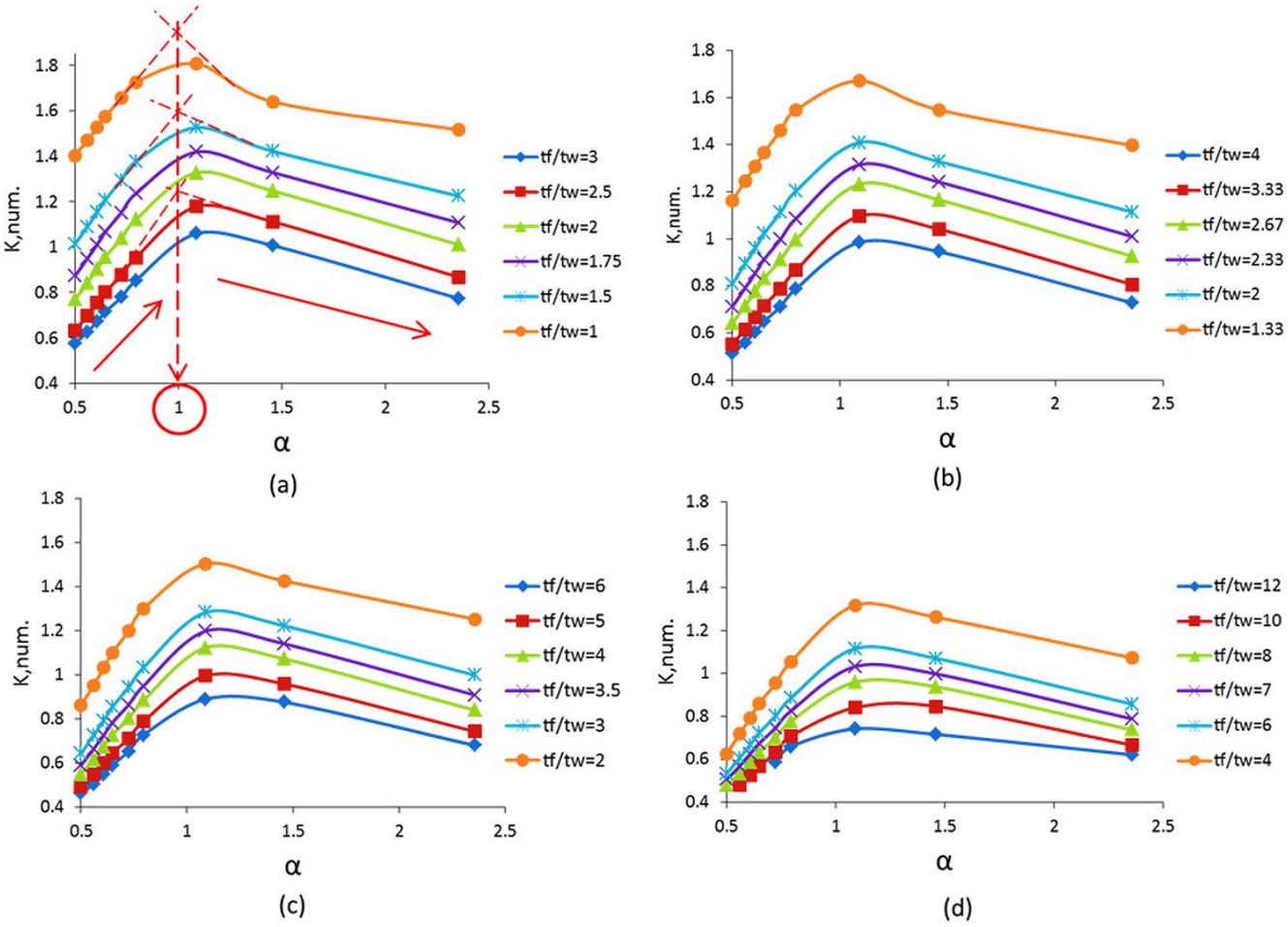

Fig. 12. Effect of panel aspect ratio: (a) $h_w/t_w = 125$, (b) $h_w/t_w = 167$, (c) $h_w/t_w = 250$, (d) $h_w/t_w = 500$.

determined according to **Eq.** (2). For the larger flange outstand, reasonable solution has been obtained. The obtained values from the numerical analysis were not related to the smaller outstand of the flange.

$$k_{\sigma,num.} = \frac{\sigma_{cr,FEM.}12(1-\nu^2)}{\pi^2.E}\left(\frac{C_f}{t_f}\right)^2 \tag{2}$$

The effects of the analyzed parameters have been evaluated considering that a_1 equal to a_2 and $\theta = 45°$. Similar tendencies were noticed in the other analyzed trapezoidal profiles.

4.1. Effect of panel aspect ratio ($\alpha = C_f/a$)

At low and high web slenderness ratio, Increasing C_f/a ratio increases the buckling coefficient effectively by mean value of 85% up to C_f/a ratio almost equal to 1, then any increase in C_f/a ratio more than 1 decreases the buckling coefficient slightly by 22%; this was due to decreasing the buckling length (a) which leads to higher buckling stress consequently higher buckling coefficient value. The results are shown in Fig. 12.

4.2. Effect of flange-to-web thickness ratio (t_f/t_w)

The main function of the corrugated web in corrugated web steel girders subjected to pure bending moment is the supporting of the flange. Increasing t_f/t_w ratio decreases the buckling coefficient effectively by 59% in small web slenderness ratio ($h_w/t_w = 125$). In higher web slenderness ratio ($h_w/t_w = 500$), a small decrease by 23% was noticed. This decrease was due to decreasing the corrugated web supporting effect and consequently decreasing the local buckling coefficient as well. The effect of web slenderness ratio was more logic as in lower h_w/t_w (higher t_w), the corrugated web working as rigid support to the flange and significantly affects on the buckling coefficient. The effect of ratio of flange-to-web thickness has been noticed clearly at t_f/t_w ratio up to 2.5, and then this effect was marginal at t_f/t_w ratio higher than 2.5 as the web has been considered as hinged support to the flange as shown in Fig. 13.

In a comparison with Jáger et al. [13], flange induced buckling, combined and separated local flange buckling are three different buckling modes of the compression flanges were parted based on the slenderness ratio of web and the flange-to-web thickness ratio. They concluded that the flange-to-web thickness ratio has a large effect on the moment capacity of trapezoidal corrugated web girders. In the current study, similar tendencies of the effect of flange-to-web thickness ratio were observed at all web slenderness ratios.

4.3. Effect of enclosing effect of trapezoidal web

At R higher than 0.14, the bending moment resistance of trapezoidal corrugated web girders has been affected by the enclosing effect of the corrugated web effectively. As increasing R more than 0.14, reduces the capacity of these girders in bending moment as shown in Fig. 14. This effect was due to that the flange local buckling of the sub-panels of the compression flange occurred in a localized manner of stress as indicated in Fig. 15. The distance between the supports of flange sub-panel increases at higher values of R, so the bending moment resistance reduced.

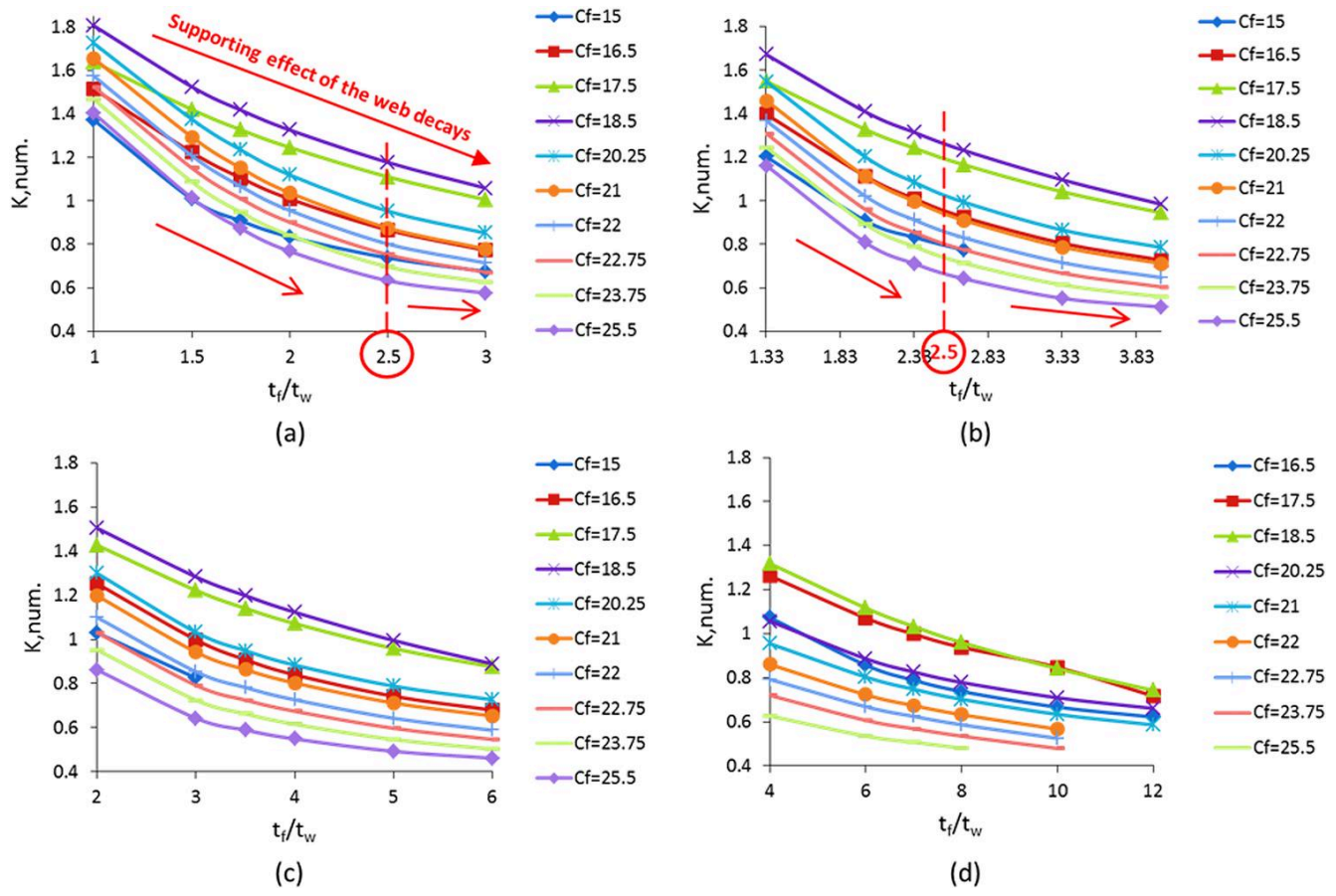

Fig. 13. Effect of flange-to-web thickness ratio: (a) $h_w/t_w = 125$, (b) $h_w/t_w = 167$, (c) $h_w/t_w = 250$, (d) $h_w/t_w = 500$.

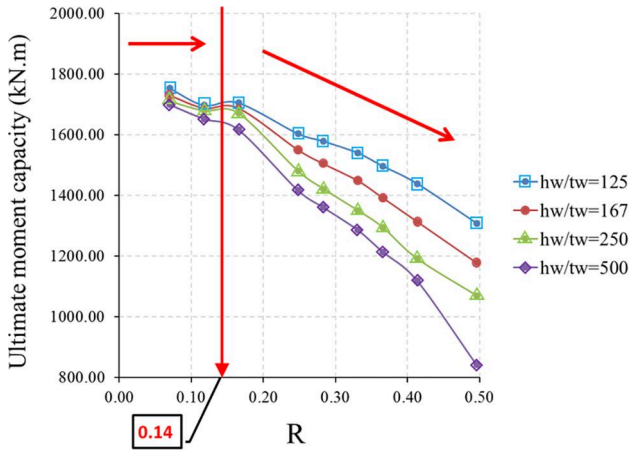

Fig. 14. Effect of enclosing effect of corrugated web.

4.4. Effect of flange slenderness ratio (C_f/t_f)

In the numerical analysis, it has been noticed that using the maximum outstand distance (C_f) in calculating the buckling coefficient lead to unreliable values. In case of higher values of enclosing effect of the trapezoidal corrugated web more than 0.14, the maximum outstand distance may be suitable to be used in the buckling stress equation (**Eq. (2)**) as the buckling occurs in every sub-panel of the compression flange. On the other side, in case of values of the enclosing effect of the corrugated web equal to or less than 0.14, the average outstand distance ($b_f/2$) can be considered as shown in Fig. 16.

As C_f/t_f increases, the buckling coefficient significantly decreases as shown in Fig. 17. In the girders having enclosing effect almost equal to 0.14, higher buckling coefficient has been obtained. Using higher C_f/t_f ratio due to using higher C_f makes the flange more slender and leads to obtain low compressive stress and consequently low buckling coefficient.

4.5. Effect of web slenderness ratio (h_w/t_w)

In high ratio of C_f/t_f more than 11, increasing the slenderness ratio of the corrugated web (h_w/t_w) is effectively decreases the bending moment capacity of such girders ($M_{ult.}$). In low C_f/t_f less than or equal to 11, increasing slenderness ratio of corrugated web (h_w/t_w) has a small effect on the bending moment capacity as shown in Fig. 18. This value of C_f/t_f has been given before by the Egyptian code as:

$$\frac{C_f}{t_f} \le \frac{210}{\sqrt{F_y}} \tag{3}$$

where f_y is the material yield stress in MPa.

It means that this equation which has been used for limiting non-compact sections can be used also to specify the range where web slenderness ratio affected on the bending moment capacity.

4.6. Proposal of new design procedure

Design of built up sections under bending moment requires non-slender flanges to be considered.

In most of the previously developed design methods for unstiffened plated elements, the relative slenderness may be calculated according to **Eq. (4)**.

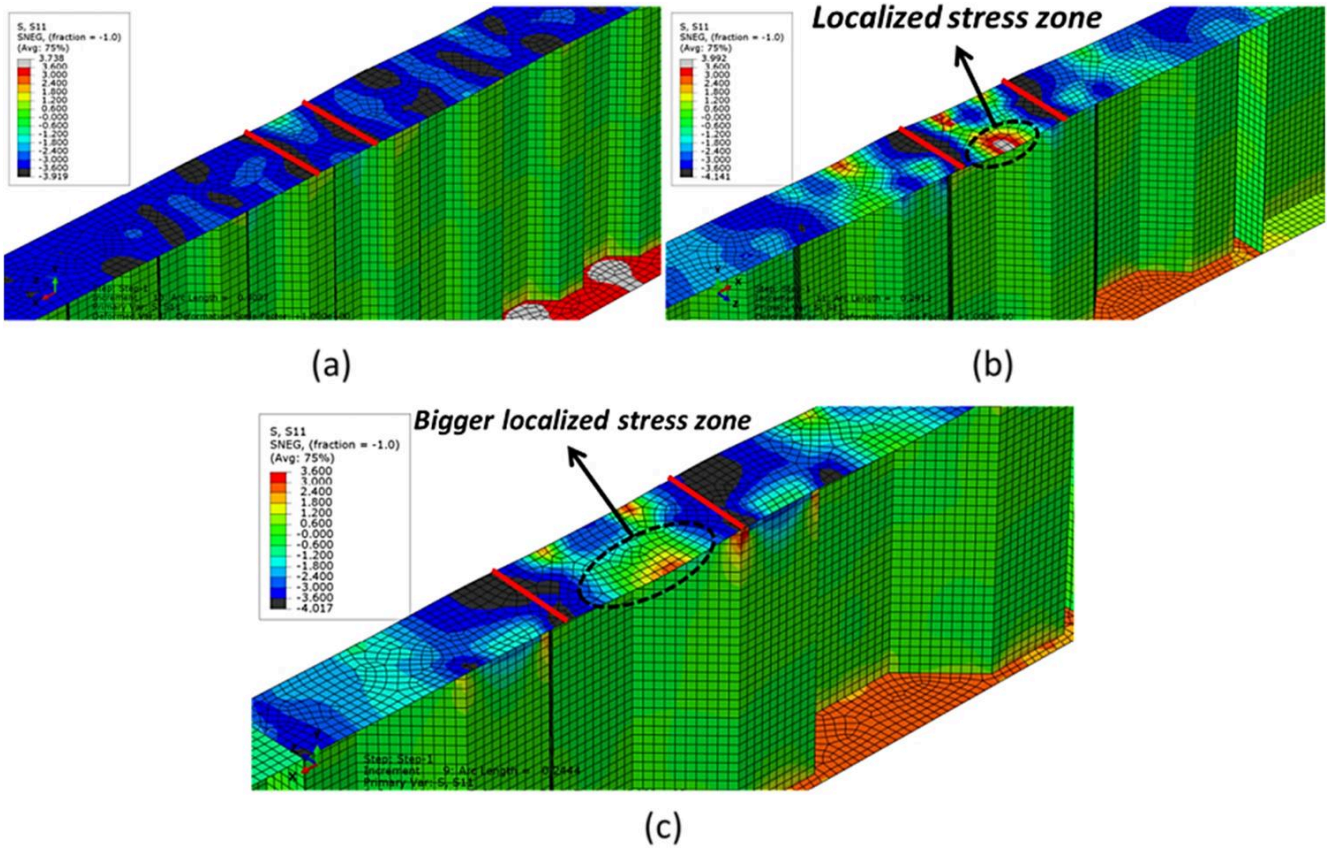

Fig. 15. Flange stress distribution: (a) R = 0.165, (b) R = 0.331, (c) R = 0.5.

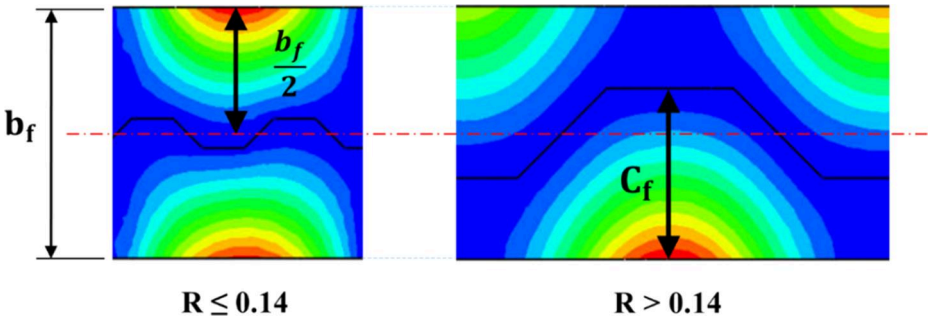

Fig. 16. Average and maximum outstand distance.

$$\lambda_p = \frac{c_f/t_f}{28.4\ \varepsilon\ \sqrt{k_\sigma}} \tag{4}$$

where $\varepsilon = \sqrt{\frac{235}{F_y}}$; F_y in MPa.

The limiting equation of Egyptian code (**Eq.** (3)) which used in classifying the non-compact flanges should be modified to be used in I-sections with trapezoidal corrugated webs. The EC3 specified the relative slenderness parameter which used in the derivation of the limiting equation.

$$\lambda_p = \sqrt{\frac{F_y}{\sigma_{cr}}} \tag{5}$$

where σ_{cr} is calculated from **Eq.** (2) and by substituting in relative slenderness parameter equation, **Eq.** (6) has been found.

$$\frac{c_f}{t_f} = \lambda_p \sqrt{\frac{\pi^2 E k_\sigma}{12(1-\nu^2) f_y}} \tag{6}$$

According to [19], in case of simply supported plate of flange (three sided plate under uniaxial compression stress), $k_\sigma = 0.425$ has been used. In case of fixed supported plate of flange, $k_\sigma = 1.28$ has been used. The AISC suggested a value of the buckling coefficient $k_\sigma = 0.7$ to be used in flange of flat web girders.

In the new suggested equation of flange local buckling coefficient in trapezoidal corrugated web plate girder (**Eq.** (7)) presented by Jáger et al. [14] in the literature, the buckling coefficient can be accurately calculated taking in consideration the effect of geometric parameters neglected before, so this new equation has been used to obtain the new design equation for flanges supported by trapezoidal corrugated web.

$$k = 0.43\left(2.5\frac{t_w}{t_f}\right)^{0.6+R} + \left(\frac{C_f}{a_1 + a_4}\right)^2 \tag{7}$$

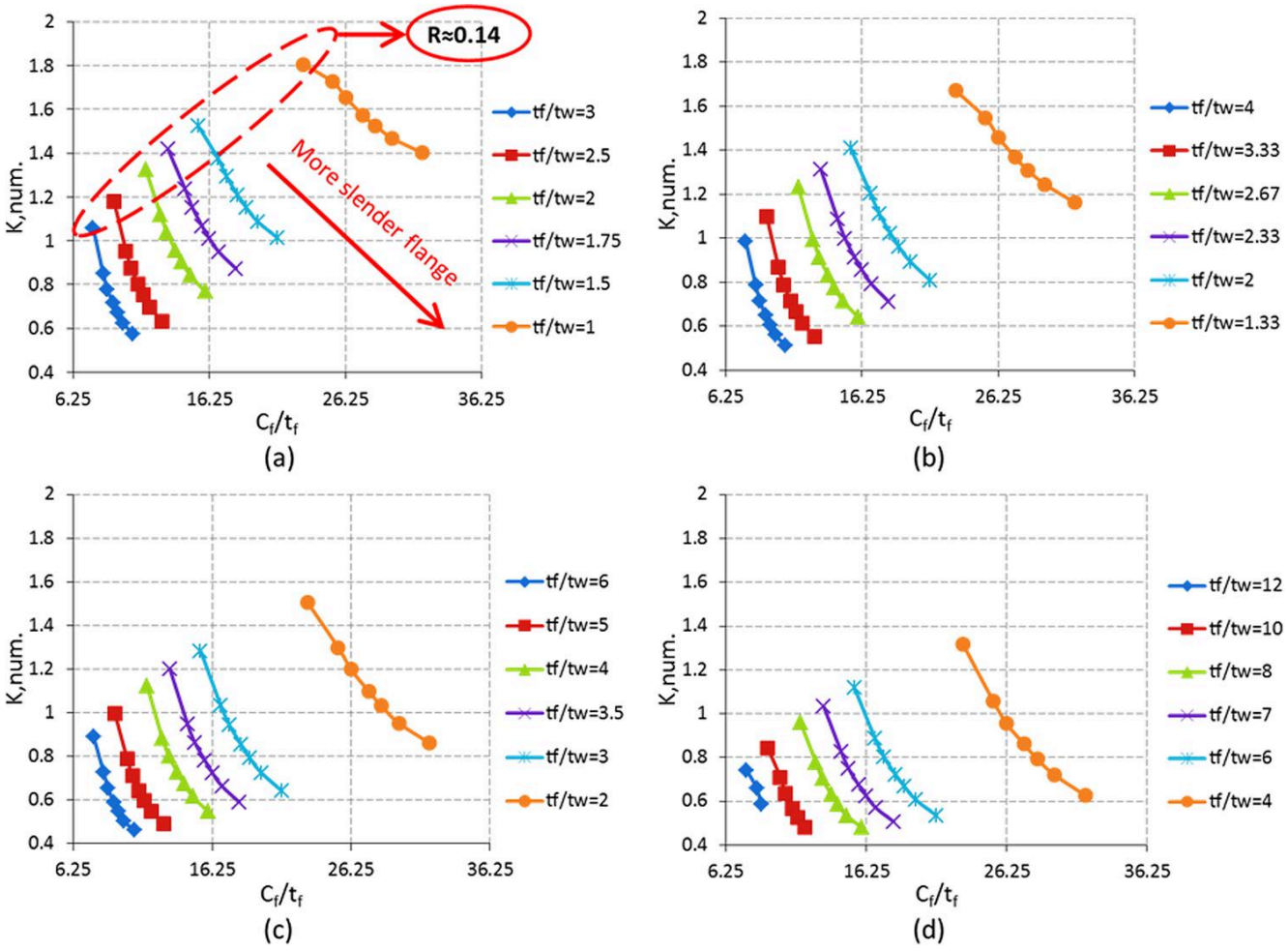

Fig. 17. Effect of flange slenderness ratio: (a) $h_w/t_w = 125$, (b) $h_w/t_w = 167$, (c) $h_w/t_w = 250$, (d) $h_w/t_w = 500$.

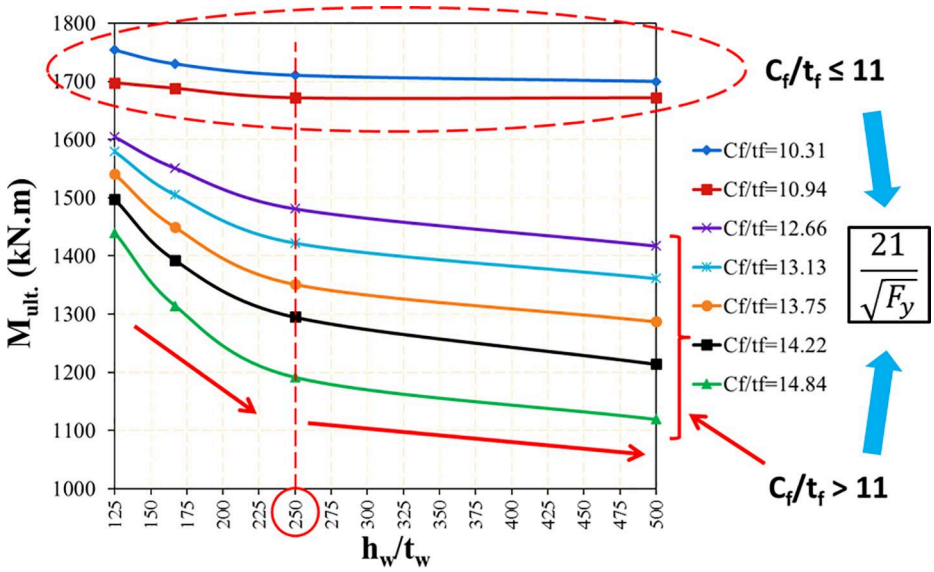

Fig. 18. Effect of web slenderness ratio on ultimate bending capacity.

Jáger et al. [14] proposed that the relative slenderness limit should be $0.493/\sqrt{k_\sigma}$ for trapezoidally corrugated web girders. In the current theoretical investigation of compression flange classification, the minimum and safe value of flange buckling coefficient could be assumed 0.43. So, the relative slenderness limit equals 0.752 according to the proposal of Jáger et al. [14]. As a results, a new equation (**Eq. (8)**) has been deduced to be used in the classification of the compression flanges in plate girders with trapezoidal corrugated web.

$$\frac{c_f}{t_f} = 0.752\sqrt{\frac{\pi^2 * 210000 * k_\sigma}{12(1-0.3^2)f_y}} = 326\sqrt{\frac{k_\sigma}{f_y}} \quad (8)$$

where k_σ is the flange local buckling coefficient obtained by the new proposed equation (**Eq. (7)**).

5. Conclusions

From the previous numerical investigations and analyses, the main conclusions of the current study have been drawn as follows:

1. Higher values by 85% of flange local buckling coefficient have been obtained at value of flange sub-panel aspect ratio almost equal to 1 than flange sub-panel aspect ratio equal 0.5.

2. Increasing flange-to-web thickness ratio decreases the local buckling coefficient of the flange effectively by 59% in small web slenderness ratio ($h_w/t_w = 125$) and by 23% in high web slenderness ratio ($h_w/t_w = 500$) up to t_f/t_w ratio equal to 2.5, and then any increase in t_f/t_w ratio has a marginal effect on the buckling coefficient.

3. The highest local buckling coefficient values of flange in trapezoidally corrugated web girders have been obtained by making the web enclosing effect almost equal to 0.14.

4. Increasing the flange slenderness ratio decreases the local flange buckling coefficient effectively.

5. The criteria classifying the flange in flat web girders given previously by the Egyptian code (**Eq. (3)**) can be used safely in trapezoidal web girders to specify the effect of web thickness on the bending resistance.

6. In the classifying of the compression flange, the maximum flange outstand should be used in trapezoidally corrugated web girders with enclosing effect of 0.14 or more. In range of enclosing effect less than 0.14, average flange outstand may be suitable to be used.

7. For economic design purposes, decreasing the trapezoidal corrugated web enclosing effect increases the bending moment resistance of these girders up to enclosing effect of 0.14, and then any decrease has almost no effect on the bending capacity.

8. At flange slenderness ratio more than 11, the bending moment capacity of trapezoidal corrugated web girders has been affected by the web slenderness ratio significantly up to web slenderness ratio of 250. At flange slenderness ratio less than 11, the effect of slenderness ratio of the web was marginal.

Declaration of Competing Interest

The authors declare that they have no known competing financial interests or personal relationships that could have appeared to influence the work reported in this paper.

References

[1] Tohamy SA, Abu El Ela OM, Saddek AB, Mohamed AI. Efficiency of plate girder with corrugated web versus plate girder with flat web. Minia J Eng Technol 2013; 32:62–77.

[2] Moon J, Yi J-W, Choi BH, Lee H-E. Lateral – torsional buckling of I-girder with corrugated webs under uniform bending. Thin-Walled Struct 2009;47(1):21–30. https://doi.org/10.1016/j.tws.2008.04.005.

[3] Johnson RP, Cafolla J. Fabrication of steel bridge girders with corrugated webs 1997;75:133–5.

[4] Elgaaly M, Seshadri A, Hamilton RW. Bending strength of steel beams with corrugated webs. J Struct Eng 1997;123(6):772–82. https://doi.org/10.1061/(ASCE)0733-9445(1997)123:6(772).

[5] Chan CL, Khalid YA, Sahari BB, Hamouda AMS. Finite element analysis of corrugated web beams under bending. J Constr Steel Res 2002;58(11):1391–406. https://doi.org/10.1016/S0143-974X(01)00075-X.

[6] Dabon M, Elamary AS. Flange compactness effects on the behavior of steel beams with corrugated webs. J Eng Sci 2006;34:1507–23.

[7] Watanabe K, Masahiro K. In-plane bending capacity of steel girders with corrugated web plates. J Japan Soc Civ Eng 2006;62:323–36.

[8] Sayed-Ahmed EY. Behaviour of steel and (or) composite girders with corrugated steel webs. Can J Civ Eng 2001;28(4):656–72. https://doi.org/10.1139/cjce-28-4-656.

[9] Ng ZL, Osman MH. Design and Performance of Steel Section with Trapezoid Web: Local flange buckling of trapezoidal web profile Analysis. Univ Technol Malaysia 2008.

[10] Lho S-H, Lee C-H, Oh J-T, Ju YK, Kim S-D. Flexural capacity of plate girders with very slender corrugated webs. Int J Steel Struct 2014;14(4):731–44. https://doi.org/10.1007/s13296-014-1205-z.

[11] DASt-Richtlinie 015. Trager mit schlanken Stegen. Stahlbau-Verlagsgesellshaft. Köln; 1990.

[12] Li GQ, Jiang J, Zhu Q. Local buckling of compression flanges of H-beams with corrugated webs. J Constr Steel Res 2015;112:69–79. https://doi.org/10.1016/j.jcsr.2015.04.014.

[13] Jáger B, Dunai L, Kövesdi B. Flange buckling behavior of girders with corrugated web Part I: Experimental study. Thin-Walled Struct 2017;118:181–95. https://doi.org/10.1016/j.tws.2017.05.021.

[14] Jáger B, Dunai L, Kövesdi B. Flange buckling behavior of girders with corrugated web Part II: Numerical study and design method development. Thin-Walled Struct 2017;118:238–52. https://doi.org/10.1016/j.tws.2017.05.020.

[15] SIMULIA. ABAQUS/standard analysis user's manual. n.d.

[16] Research Center for Housing and Physical Planning in cairo. Egyptian Code of Practice for Steel Construction and Bridges. vol. No.451. 2008.

[17] Hassanein MF, Elkawas AA, El HAM, Elchalakani M. Shear analysis and design of high-strength steel corrugated web girders for bridge design. Eng Struct 2017;146:18–33. https://doi.org/10.1016/j.engstruct.2017.05.035.

[18] European Committee for Standardization. EN 1993-1-5: Eurocode 3: Design of Steel Structures. Part 1-5: Plated Structural Elements. vol. 3. 2007.

[19] Timoshenko SP, Gere JM. Theory of elastic stability. New York, Toronto, London: McGraw-Hill Book Company; 1961.